Creation of a Laser Desorption Source for C_{60} Buckminsterfullerene

by

Andrew Scheck

A thesis submitted to the

Faculty of the College of Arts and Sciences at

the University of Colorado Boulder

in partial fulfillment of the requirements for

Undergraduate Departmental Honors in the

Department of Physics

April 10, 2023

Committee Members:

Jun Ye, Department of Physics, Thesis Advisor

John Cumalat, Department of Physics

Rainer Volkamer, Department of Chemistry

Scheck, Andrew (Undergraduate honors)

Creation of a Laser Desorption Source for C_{60} Buckminsterfullerene

Thesis directed by Prof. Jun Ye, Department of Physics

Buckminsterfullerene or C_{60} is a molecule with many interesting properties that has garnered extensive study. Ongoing research into the interesting physics present in the molecule utilize gas phase C_{60} to conduct resolved state spectroscopy. Currently, the biggest limitation on these experiments is the large heat load intrinsic to the method of gas production. This thesis presents an alternative to the current method of gas production. This new method utilizes laser desorption in order to produce gaseous C_{60} while maintaining a minimal heat load on the system. Two different ways of utilizing laser desorption have been tested, and the results of both are presented here. The results obtained show promising evidence for the validity of laser desorption as an improved C_{60} gas source, although further research to verify certain aspects of the gas produced by laser desorption is necessary.

Acknowledgements

I would like to acknowledge the support and guidance of Professor Jun Ye. Thank you for setting me on this path, and giving me the support necessary to excel in my studies and research.

Additionally, I would like to give a very large acknowledgement to Dr. Lee R. Liu. Without your teaching and help I wouldn't have been able to accomplish anything. Thank you for all the skills you've taught me and for teaching me what it means to be a physicist.

Finally I would like to acknowledge my father. Thank you for both pushing me and supporting me when I needed it.

Contents

Chapter

Figures

Figure

Chapter 1

Introduction

Buckminsterfullerene or C_{60} has garnered much interest and study since its discovery in 1985 by Kroto, Smalley and Curl. [16]. The molecule was initially studied due to the interesting properties that may arise due to its highly symmetric nature. In addition to this, potential industrial applications were sought and its presence in interstellar dust became immediately apparent after deeper study of the molecule [10] [6] [14].

Currently in the Ye lab, research into C_{60} has turned to studying the rovibrational quantum states of the molecule. These studies hope to probe the many-body physics of strongly interacting systems, such as large molecules. The main method of study to probe these physics is through resolved state spectroscopy [2]. Spectroscopic studies of C_{60} have one major limitation due to the fact that the C_{60} must be sufficiently cold. Resolved state spectroscopy requires exciting rovibrational states from a thermal ground state, so the gas being studied must be sufficiently cooled to maintain the ground state. Specifically, the C_{60} being studied must have an internal energy below the lowest vibrational excited state at 391 K [9]. Because C_{60} is a solid at room temperature but must be in a gas phase to perform these studies, this presents a large challenge that limits the efficacy and accuracy of such experiments. Due to the large size of C_{60} physical methods of cooling must be utilized in

order to reach temperatures that keep C_{60} in the thermal ground state. These methods currently center around collisional cooling with inert gasses, also known as buffer gas cooling [7].

The main source of thermal energy input into C_{60} experiments arises from the method of sublimating the particles from a solid powder into a gas. Current experiments utilize a copper oven attached to a chamber containing the buffer gas. In order to sublimate the C_{60}, the oven must reach temperatures of 800-950K [11], while the buffer gas must cool the C_{60} to temperatures less than 150K [2]. To get a sufficient flux of C_{60} the oven must be within millimeters of the buffer gas chamber, which produces a large heat load on the system. Thus, in order to minimize the heat input the most obvious improvement would be replacing the oven.

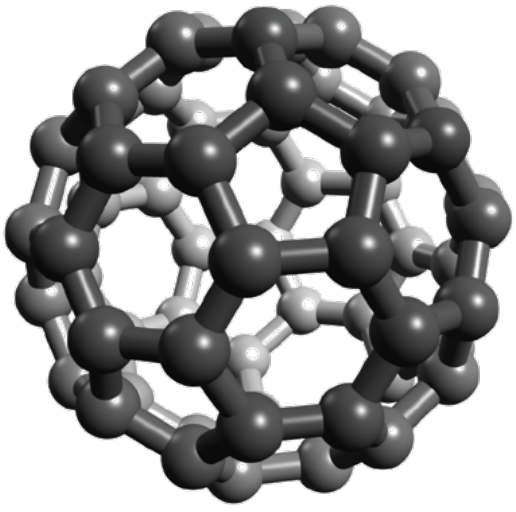

Figure 1.1: Artistic rendering of a C_{60} molecule. [Image credit: Bryan Changala].

To this end I have tested and developed an alternative method of producing gaseous C_{60}

utilizing laser desorption. Chapter 2 will go further in depth on the history and importance of C_{60}, and the theory behind desorption and its relevance to C_{60} production. Chapter 3 will shift focus and discuss the bulk of the research conducted for this thesis. This chapter will discuss the exploration of back desorption and front desorption. Chapter 4 will present the major some brief conclusions and a summary of the results. Chapter 5 will suggest some avenues for future research based on the findings in this thesis.

Chapter 2

Background

2.1 Buckminsterfullerene, C_{60}

Buckminsterfullerene or C_{60} was first discovered by Kroto and Smalley et. al in 1985 [16]. They identified a molecule which contained 60 carbon atoms through the use of mass spectrometry on gas produced by ablating graphite rods. Because mass spectrometry only shows the mass to charge ratio, a structure could only be guessed at this point. Kroto and Smalley's discovery proved the existence of C_{60}, but large quantities couldn't be synthesized until 1990 [5].

Following the discovery of methods to produce large quantities of C_{60}, interest in the molecule grew rapidly. The main feature of interest in C_{60} is its spectacular symmetry. Because of the regularity in its shape, C_{60} is incredibly stable for such a large molecule. Additionally, because of the layout and structure of its bonds C_{60} exhibits many interesting properties, mainly due to the presence of free electrons in the molecule. These properties have made C_{60} an interesting candidate for increasing efficiency in solar cells [3] as well as having the potential to be a strong superconductor [14]. Additionally, because of its rigidity and the presence of free electrons, C_{60} is an ideal candidate for studying many body physics

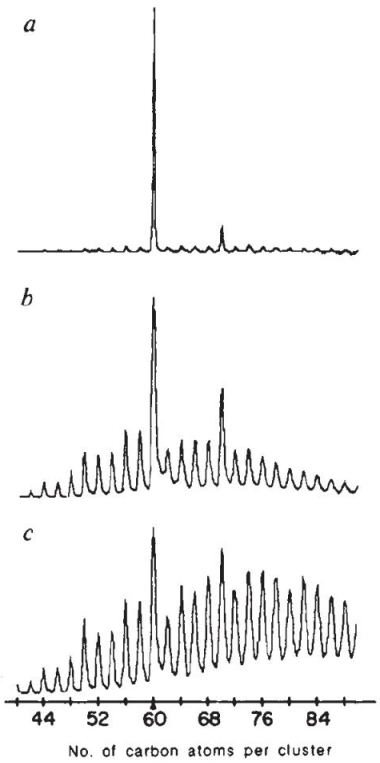

Figure 2.1: The original mass spectrometry results showing the presence of a molecule with 60 carbon atoms. Image credit: [16].

[7].

2.1.1 C_{60} as a Many-Body System

Quantum Many-body physics is the study of particles interacting within the quantum regime. That is, many-body physics probes the way wave-like particles interact with each other. Many-body physics can explain many physical phenomena such as superconductivity, current flow, and Fermi gases. We hope to use C_{60} as a model to investigate behaviour that arises specifically from interactions between the constituents of a system, rather than the constituents themselves.

Experiments to study many-body systems generally create well-ordered multi-particle

systems out of small particles, typically ultra cold molecules, held within potential wells. Experiments are generally engineered in this way because small particles are well understood and easily manipulated.

Specially engineered systems made up of isolated particles are not the only many body systems that exist. In fact, large molecules are naturally occurring many-body systems due to the presence of relatively large numbers of atoms interacting with each other through covalent or dispersive bonds. Unfortunately, most large molecules are inadequate for precise many body experiments due to intrinsic spectral broadening and congestion [12]. Many-body experiments hope to put systems in very specific quantum states in order to study them. This is simple to do for engineered lattices of isolated particles, but large molecules often have states that blur together making it impossible to gain any information from them. The blurring of states is due to the large density of states at high internal excitation, which broaden spectral features through intramolecular coupling. Additionally, to excite specific states the system must start in the ground state, meaning the particles must be sufficiently cooled to eliminate any rotational or vibrational energy present. For small particles this is easy to do using laser cooling, but cooling large molecules this way is virtually impossible. This makes large molecules generally bad systems to study many-body physics on.

Surprisingly, C_{60} breaks both of these rules: it has well defined ro-vibrational states due to its strong symmetry and rigidity, and due to their stiffness, a large fraction of molecules occupy the vibrational ground state even at a relatively high temperature. Because of these features, C_{60} presents an ideal candidate for experimenting on a molecular many-body system. Because of its incredibly symmetric shape the properties of the system are predictable,

allowing us to create models and test hypotheses about the system. Additionally, the rigidity of the molecule's bonds keep the shape of the particles relatively fixed across the range of rotational and vibrational states. This gives rise to very well resolved energy levels that do not blur together and can be excited using resolved state spectroscopy.

In current experiments on C_{60}, a laser with a precisely known frequency is directed onto a sample of gaseous C_{60} in order to excite specific states. The laser is incident on a photodetector which will show a drop in signal from the baseline of a complete lack of C_{60} if any of the light is absorbed by the C_{60}. Thus, sweeping the laser over a range of wavelengths reveals where C_{60} absorbs light to jump into a higher energy level, revealing a well defined absorption spectrum. A small portion of the absorption spectrum of C_{60} can be seen in figure 2.2. The peaks in the spectrum show quantum states being excited across a range of energies. The discrete nature of these peaks is indicative of the well defined states present in C_{60} due to the molecule's symmetry and rigidity. The top axis shows the quantum number, J, which indicates the energy of the state corresponding to the energy shown on the bottom axis as the frequency of the probe laser, expressed in wavenumbers (cm^{-1}). The regular progression of rotational lines with J indicates that C60 behaves like a rigid rotor in spite of its size. C_{60} presents a system that is readily available, easily producible, and, because of these intrinsic properties predictable over a wide range of energies.

Despite C_{60} having many features that make it ideal for experiments in many-body physics, the necessary conditions for these experiments pose challenges that limit the resolution and accuracy of results. The main limitation on C_{60} experiments is the method of producing C_{60} gas. Current experiments use single molecules of C_{60} and probe the inter-

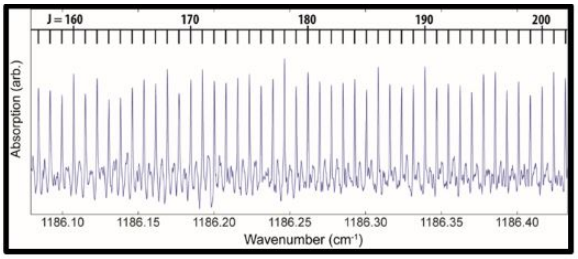

Figure 2.2: A small section of the absorption lines of the C_{60} spectrum. The discrete nature of the lines shows how a high resolution can be obtained and specific excited state energies can be determined. Image credit :[2].

actions between the atoms within those molecules. In order to obtain isolated particles of such a large molecule, a gas of C_{60} must be produced. Since C_{60} is a solid a room temperature, this means a sample must be heated before experiments can be performed. But, as mentioned previously, studies probing many-body physics must start in the ground state, which requires them to be cooled below a certain threshold. Currently, gas phase production is done by sublimating solid C_{60} powder in a copper oven. The oven must be above the sublimation point of C_{60} at around 800-950 K, the ground state of C_{60} is populated when the molecules are below 150 K. Figure 2.3 shows the importance of temperature in spectroscopic studies of C_{60}. Panel (a) shows the average vibrational energy and partition function of C_{60} as a function of temperature. The ground state exists below the point where average vibrational energy drops steeply, roughly 150 K. Panel (b) shows three different absorption spectra for C_{60}. The black spectrum shows the predicted spectrum, the blue shows an experimental spectrum of cooled C_{60}, and the red shows an experimental spectrum of hot C_{60}. The appearance of discrete absorption lines only at low temperatures is apparent. In order to improve upon this limitation, This thesis present an alternative to the oven method utilizing a technique known as laser desorption

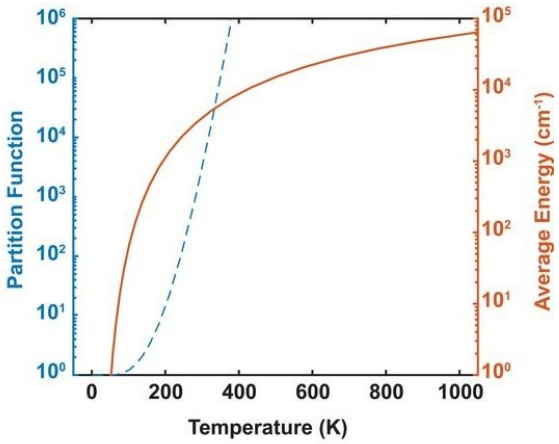

(a)

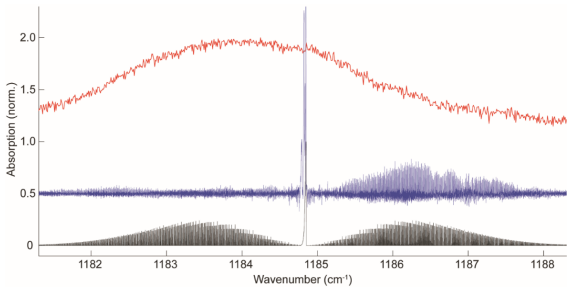

(b)

Figure 2.3: (a) The average vibrational energy and partition functions of C_{60} as a function of temperature. The drop to 1 in the partition function at roughly 150 K shows that most of the C_{60} will be in the ground state below that temperature. (b) Three absorption spectra of C_{60}. The black spectrum is the theoretical absorption spectrum, while the red and blue are determined experimentally. The red spectrum is from C_{60} gas at roughly room temperature, and the blue is cooled C_{60} so that the starting state of the system is the ground state. Credit for both: [2].

2.2 Desorption

The main purpose of laser desorption is to isolate molecules by inputting energy, breaking the intermolecular bonds present in the solid phase. There are two types of desorption, thermal and laser desorption. Thermal desorption involves directly heating the target to break bonds, while laser desorption utilizes specific wavelengths that can be absorbed by the desired molecule, or analyte, to input energy. This thesis will focus on laser desorption since it was the main method tested. There are several benefits of laser desorption. Namely, laser desorption requires minimal setup within the environment where the experiment takes place, it produces gas nearly instantaneously, and has a very low heat load. In contrast, can take up to an hour to start producing gas, and have a very large heat load, putting limitations

on experiments.

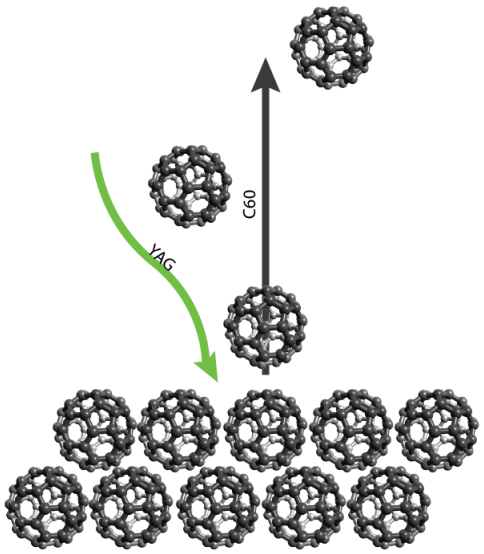

Figure 2.4: The most basic laser desorption setup. A laser (generally a Nd:YAG laser, or YAG in the figure) hits a target of the desired molecule (C_{60}) and provides enough energy for some of the particles to escape the solid into the gas phase.

Laser desorption is commonly used in biochemical studies [1]. In principle, desorption can produce isolated molecules without any excess energy being put into the molecules. For delicate molecules, this means there is a very good chance the molecules to be studied will maintain their integrity without undergoing undesirable chemical changes. In this thesis, I show how many of the methods used in biochemical studies can be adapted to C_{60} with the hope of avoiding disadvantages associated with oven methods of gas production.

When used for biochemical samples the analyte is generally deposited onto some substrate. The choice of substrate often depends on the properties of the analyte. There must be some adhesion between the substrate and the analyte, but in order to maintain the integrity of the analyte they cannot react with each other. Common substrates include graphite, silicon, and many metals. In order to deposit the desired analyte on to the substrate many

different techniques can be used. These include physical vapor deposition, evaporative coating, and hydraulic pressing of the analyte (hydraulic pressing may not use a substrate in some cases). Physical vapor depostion is the process of sublimating or vaporizing the analyte which then condenses on a substrate kept at a lower temperature. In this case, the substrates are often large, solid, disks. Once the substrates have been coated with the analyte, they can be used as targets for laser desorption by heating either the substrate or the analyte directly. Physical vapor deposition is covered in depth in section 3.1.1.1 and the differences in heating the substrate versus the analyte is covered more in depth in sections 3.1 and 3.2.

Alternatively, if the analyte is easily dissolvable in volatile solvents, evaporative coating provides a simple and effective method of coating substrates. Evaporative coating consists of dissolving the analyte in a volatile solvent which is then poured on top of a solid substrate. The substrate serves as a seed for crystals of the analyte to form as the solvent evaporates. The analyte forms thin layers over the rigid, solid substrate, creating a target for desorption. There are several different ways evaporative coating can be done besides simply pouring the solution onto the substrate. These include spraying the solution onto the substrate with an atomizer in order to produce a very thin layer, or putting a small amount of solution onto the substrate and spinning it very fast in order to produce a very uniform film. Both of these alternative methodologies are useful for forming thin films, ideal for when only small quantities of the analyte can be obtained.

Another method of producing targets is hydraulic pressing. Hydraulic pressing is generally used when the analyte is readily available and larger amounts are desired for the experiment. A hydraulic press is used to compress the analyte, generally in a powder form,

into a solid disk. The analyte can be compressed with or without a substrate. When compressed without a substrate, the analyte forms a solid, standalone disk that can be laser desorbed. When using a substrate, the analyte is pressed into the substrate, also known as a backing plate in this case. The analyte may also be mixed with binding agents before hydraulic pressing. Binding agents are useful to lower the amount of analyte necessary to form a desorption target, as well as aiding in adhering the analyte either to itself or the backing plate. Any binding agents included must not be able to react with the analyte. Common binding agents are graphite and various metals such as bismuth.

Binding agents can also be used to aid in the desorption process. It is possible to use a specific wavelength for laser desorption that the binding agent absorbs but the analyte does not, causing the binding agent to heat up and locally thermally desorb the analyte. This method has the lowest probability of fragmenting the analyte, but it is often hard to find a wavelength that is only absorbed by the binding agent. Each of these target production methods (physical vapor deposition, evaporative coating and hydraulic pressing) have been tested. The results and deeper discussion on the methods themselves are shown in section 3.

Chapter 3

Desorption Tests

3.1 Back Desorption

Back desorption involves using a laser to sublimate an analyte by heating a substrate to some critical temperature. The substrate is coated on one side with the analyte and the opposite side is hit with a focused laser beam, locally heating up the substrate in order to sublimate the analyte into a gas. This avoids exposing the analyte to a high-powered laser directly, which may reduce undesired chemical reactions.

3.1.1 Target Preparation

Targets for back desorption were made using stainless steel foils as a substrate material, coated with the C_{60} analyte to be desorbed. Various thicknesses of foils were tested and several methods of applying C_{60} onto the foils were tested. Stainless steel was chosen as the substrate because C_{60} readily adhered to it in earlier experiments [17]. Decisions regarding the quality of the targets were made using qualitative observations of observed thickness, relative brittleness, and crystal uniformity. The desired properties were thick, uniform, non-brittle films of C_{60}. Thickness is important in order to maximize the yield of C_{60} from a single target. Additionally, a uniform coating is assumed to minimize the variance in desorbed C_{60}

between laser pulses. Finally, with our current setup, finished targets must be moved from the chamber used for production to a separate chamber for experiments. This makes non-brittle targets preferable so they are less likely to break in transit. To coat the foils physical vapor deposition and evaporative coating methods were both tested.

3.1.1.1 Physical Vapor Deposition (PVD)

Figure 3.1 shows the setup utilized for physical vapor deposition to coat the stainless steel substrates. The oven (left) is made of copper and is used to sublimate the C_{60} at a temperature of 900 ± 25 K. The oven consists of two SiN igniters which heat a crucible filled with C_{60}. The heaters (white Rodgers 768A-842 SiN igniters) are positioned on opposite sides of the crucible to evenly heat the oven. The oven can be seen in figure 3.2. This is then loosely covered with a copper foil heat shield in order to minimize the amount of heat lost to radiative cooling, and shield the rest of the chamber from radiative heating.

The stainless steel substrate is held in a mount situated in the center of the chamber. The mount is held in thermal contact with the exterior of the chamber through a metal rod to maintain a cooler temperature on the foil. The chamber is evacuated to a pressure of 7 mTorr using a low speed turbomolecular pump and is then flooded with 250 mTorr N_2 gas in order to purge the chamber. The inert atmosphere is also believed to aid in crystal growth as found in [8], potentially creating thicker films.

The igniters are powered by a variac transformer in order to maintain constant current and thus a fixed heat output. The inclusion of a temperature servo to actively stabilize the oven temperature was tested as well, although it was decided that the servo was not

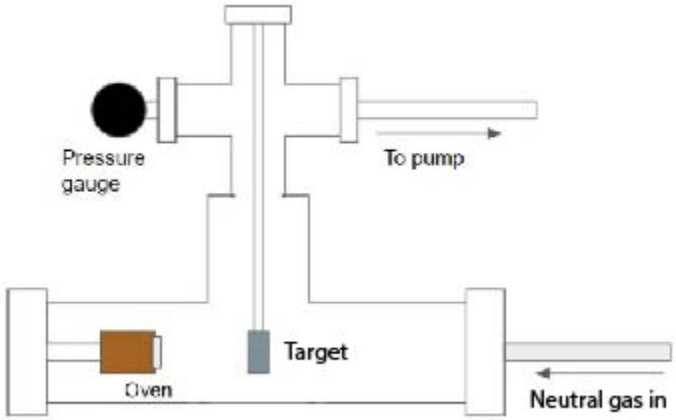

Figure 3.1: A diagram showing the setup utilized for physical vapor deposition onto stainless steel substrates. C_{60} is sublimated from the oven, which is made of copper and is heated using SiN igniters. The stainless steel substrate is placed in the center of the chamber for the C_{60} to condense onto.

useful for this particular application. Unfortunately, the servo is meant to output a specific voltage instead of a current. The igniters have a resistance proportional to temperature and so outputting a constant voltage will not maintain a steady current. The relationship between the resistance of both igniters and the oven temperature is shown in figure 3.3. This made the heating inconsistent and hard to control when using the servo because the output current would constantly change. So, we opted to use the variac transformer directly and maintain the temperature by careful monitoring and adjustments made by hand. This does not require a very complicated procedure since the oven has a high thermal mass and its temperature is already passively quite stable.

It was quickly found that C_{60} accumulated on the walls of the chamber after being sublimated in the oven. This layer of C_{60} caused the temperature of the oven drop over time, despite constant heat output by the SiN igniters. It's assumed that this is due to the

Figure 3.2: The oven used to sublimate C_{60} for PVD.

C_{60} acting as an ideal black body and absorbing heat radiatively from both the crucible and the igniters instead of reflecting it back. In order to minimize this effect, the oven was covered in a thin copper foil, as mentioned previously. In addition, a removable stainless steel "drip tray" was added to the bottom of the chamber. The "drip tray" is a piece of flexible stainless steel which can collect the excess sublimated C_{60}. The tray is removable and can easily be cleaned with solvents in order to maintain a clear inner chamber surface, mitigating radiative heat transfer, as well as minimizing C_{60} buildup.

One main issue present in the PVD setup is an "exploding" effect. Seemingly unpredictably the C_{60} will sometimes burst out of the oven all at once. We inferred that this happens due to observations of powdered C_{60} on the oven and targets. The powdered C_{60} is clearly distinct from the condensed C_{60} since it does not stick to the walls and has a matte black and dusty appearance in contrast to the shiny and smooth appearance of the condensed C_{60}. On several occasions, solid C_{60} condensates have also been observed forming over the opening of the oven. The oven exploding during target production prevents a uniform film on the stainless steel from forming, making these targets useless. Attempts to predict the "exploding" effect include varying the mass of C_{60} in the crucible as well as the oven temperature and coating time. The most effective method of minimizing "explosions" is to decrease the amount of C_{60} in the oven. It was found that 0.05 g of C_{60} kept the frequency of "ex-

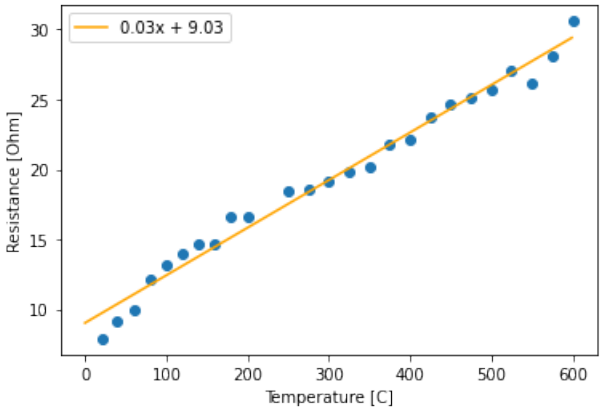

Figure 3.3: Resistance vs. temperature curve for the SiN igniters on the C_{60} oven. The curve was produced experimentally using the construction shown in in figure 3.2. A linear fit is included in order to predict the resistance based on oven temperature.

plosions" to a minimum, although it did not completely eliminate them. Several trials still had "explosions", but it's estimated that the frequency was decreased from 2 "explosions" out of 4 trials when more than 0.05 g of C_{60} was used to less than 1 out of 4 trials with at most 0.05 g of C_{60} used. Only rough scans of mass dependence were done, so it is possible that there exists some ideal mass that eliminates the explosions entirely, but it is outside the scope of the results presented here.

PVD coating creates crystalline layers of C_{60} on the substrate surface. These can be seen easily with an optical microscope. As mentioned previously, crystal uniformity would hopefully allow for thicker crystals to be grown, as the layers could build upon each other forming thick, rigid films. Changes to the coating procedure such as increasing the time to achieve the desired temperature helped improve uniformity. Despite this it's common to produce multicrystalline targets. Possible reasons for the non-uniformity are inconsistencies in temperature across the substrate causing different crystal structures to form as well as differences in the amount of sublimated C_{60} hitting certain parts of the target. An

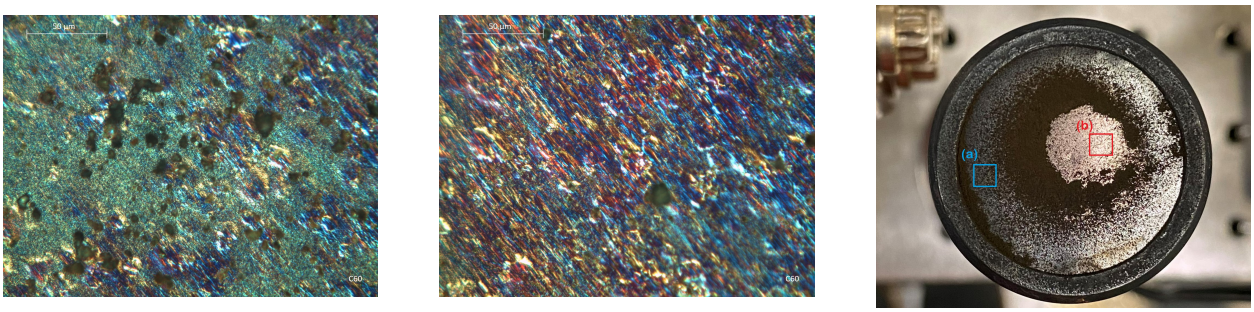

(c)

Figure 3.4: Two types of crystals can be seen, both images are taken from the same target. Image (a) shows crystals formed in small cubic blocks, while image (b) shows smooth crystals formed in striated bands. Image (c) shows the entire target.

example target with different crystals on it can be seen in figure 3.4. Figure 3.4(c) shows how differences in C_{60} concentration across the target may cause the discrepancies in crystal formation. The excess C_{60} in a ring around the center makes it clear that there was more C_{60} incident on this section of the target. This C_{60} is not attached to the target the same way as the crystals in 3.4(a) and (b) are, instead it's more like a dusty coating that falls off due to gravity when the target is inverted.

The inconsistencies in crystal formation, the "exploding" effect, and difficulties in keeping consistent heating conditions throughout trials keep PVD from being the best method for coating back desorption targets. Despite being inconsistent, the targets produced from PVD are very rigid and can be transported easily without breaking. It's possible then that lessons from PVD can be applied to other methods in order to produce a composite method that eliminates the inconsistencies, but maintains the strength of targets.

3.1.1.2 Evaporative Coating

Another method tested for producing back desorption targets is evaporative coating. Evaporative coating is done by dissolving the desired molecule in a volatile solvent. The solution is poured onto a substrate and allowed to evaporate, leaving behind a film of the solute on the substrate. In our case, a lens tube was utilized in order to hold a solution of toluene and C_{60}. A very basic diagram can be seen in figure 3.5. Toluene was used due to its availability and the relatively high solubility of C_{60} in it [15].

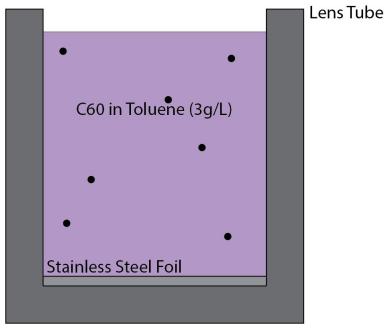

Figure 3.5: Diagram showing the evaporative coating setup.

Making the toluene-C_{60} solution at or below the saturation point produced a very thin film. An upper bound for the thickness of this film can be found by assuming all the material in solution is deposited uniformly on the substrate:

$$m_{C_{60}} = (2.8 \text{ mg/mL}) \cdot V \tag{3.1}$$

$$V_{C_{60}} = \frac{m_{C_{60}}}{\left(1.7 \times 10^3 \text{ g/cm}^3\right)} \tag{3.2}$$

$$\tau = \frac{V_{C_{60}}}{\pi(1.123 \text{ cm})^2} \tag{3.3}$$

Where V is the volume of toluene solution in mL, $m_{C_{60}}$ is the mass of dissolved C_{60} in mg (with 2.8 mg/mL being the solubility of C_{60} in toluene [15]). $V_{C_{60}}$ is the volume of solid C_{60}

in cm^3 assuming 100% of C_{60} is precipitated out (with 1.7 g/cm^3 being the density of solid C_{60}). Assuming the precipitate forms a uniform cylindrical layer the same diameter as the inside of the lens tube, the thickness of the film, τ, can be found simply by dividing the volume by the surface area of the inner diameter of the lens tube. For reasonable volumes of toluene solution (1.25 mL to fill the lens tube used) this produces a film with a maximum thickness of 0.52 μm. Estimates made for the PVD targets based on relative size of the C_{60} film compared to the stainless steel foil (thickness of 12.7 μm) gave a thickness on the order of 10^1 - 10^2 μm. This is estimated by comparing the thickness of the entire target to one of the uncoated foils. This is simple to do just by placing the two next to each other and approximating the relative increase in size of the coated foils. An optical profilometer was used to try and measure thickness as well. But, the rough surface of the targets causes the light from the profilometer to be reflected randomly and prevents the profilometer from being able to take complete data from the targets, making measurement uncertainty very large. So, measurements from the profilometer were not used. Because the evaporative coating films produced this way are so much thinner, using this evaporative coating setup is certainly not worthwhile when trying to optimize thickness.

Although coating the foils with saturated (or under-saturated) solutions is not worthwhile, it is possible to coat foils using over-saturated solutions. This is done simply by adding more C_{60} than can possibly be dissolved by the amount of toluene used. Not very many tests were done this way, but the results were promising. An example of a target produced in this manner can be seen in figure 3.6, the impressive thickness is apparent. It is hard to know the amount of C_{60} used in the solution poured onto the steel foil since the toluene and C_{60} must

be mixed in a separate container and poured over the foil. In the case of an over-saturated solution there is still solid C_{60} present after doing this, some of which gets stuck to the sides of the mixing container when pouring into the lens tube. So, measuring the exact amount of dissolved and non-dissolved C_{60} poured onto the foil is practically impossible when using this method making it imprecise and non-reproducible. So, despite the impressive preliminary results more work would have to be done in order to utilize this method for proper study.

Figure 3.6: A target produced using an over-saturated C_{60}-toluene solution

3.1.2 Desorption Tests and Yield Characterization

Desorption was performed using a 445 nm continuous wave (CW) diode laser focused onto the back of the stainless steel substrate. The peak power used was 750 mW. Desorption trials were performed both in and out of an evacuated chamber. The desorption setup can be seen in figure 3.7.

Qualitatively, desorption did appear to happen when the target was hit by the laser. This can be seen in figure 3.8, where a target is shown with multiple depleted holes in the C_{60} film where the laser beam hit.

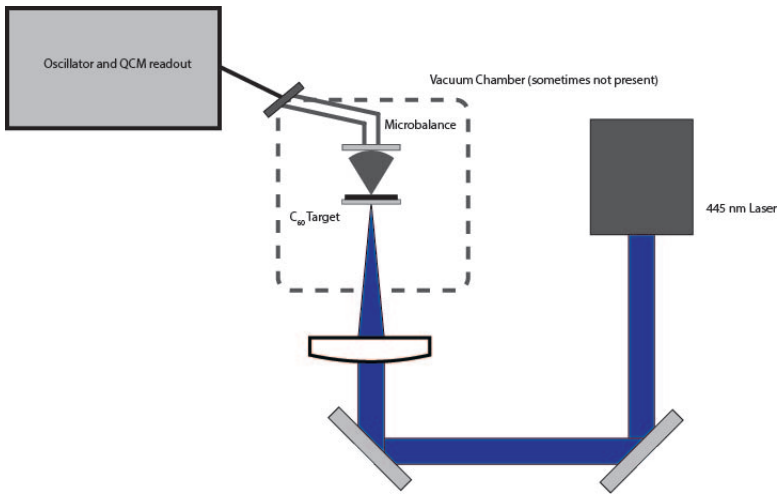

Figure 3.7: The setup for tests performed on the back desorption C_{60} Source. This configuration is using the QCM for measurements. Tests were performed both inside and outside of a vacuum chamber.

The goal of the desorption setup is to produce gaseous C_{60}. To that end, the output gas from desorption must be analyzed and the presence of molecular C_{60} must be verified. When desorbing molecules there is always the possibility of fragmenting them by breaking the intramolecular bonds, forming different compounds that are not useful for the experiment. Direct absorption spectroscopy and a quartz crystal microbalance (QCM) were used to analyze the output. The goal of using the QCM was to determine the mass of the output from the desorption source, however this has no way of determining the chemical species. On the other hand, direct absorption spectroscopy can verify the presence of C_{60} from the absorption spectrum.

The smallest measurement that can be given from the microbalance and oscillator readout used (Inficon SQM-160) is a deposited film of 1 Å(The oscillator readout only gives a measurement of film thickness or oscillator frequency shift). The thickness of the film is determined by the QCM readout using a specific density for the deposited material input

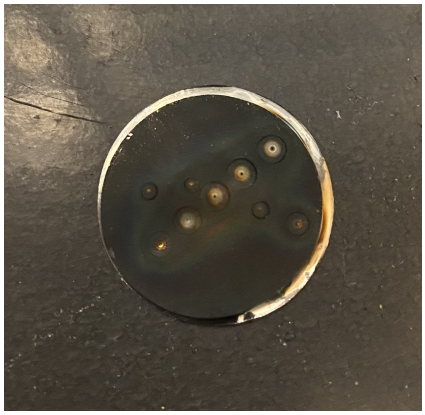

Figure 3.8: A target after back desorption tests.

into the readout. The face of the oscillator that can be coated is 12.7 mm in diameter. Using 1.7 g/cm^3 as the density of C_{60}, this gives a resolution of 21 ng of C_{60} deposited onto the oscillator, assuming all the desorbed material is in fact C_{60}. The QCM oscillator was positioned less than 1 cm in front of the C_{60} target in order to capture as much of the desorbed material as possible. Despite this, the QCM did not show any detectable response to the desorbed material, implying that only a very small amount of material was being desorbed.

The quartz crystals used in the QCM come in a variety of coatings for various applications (gold, silver, and an alloy of the two). Crystal coating is generally chosen based on whether or not the material will adhere to the crystal coating. Gold is the manufacturers recommended coating for depositing carbon based compounds. But, it has not been specifically verified that C_{60} will stick. So, further tests could be performed utilizing different crystal coatings in order to verify the results found here.

In addition to the QCM a simple absorption spectroscopy setup was made in order to have greater sensitivity to desorbed C_{60} coming off the target. Spectroscopy was done using

a 265 nm diode laser. 265 nm was chosen because of the presence of a strong absorption peak for C_{60} at that wavelength [13]. The relevant part of the C_{60} absorption spectrum can be seen in figure 3.9.

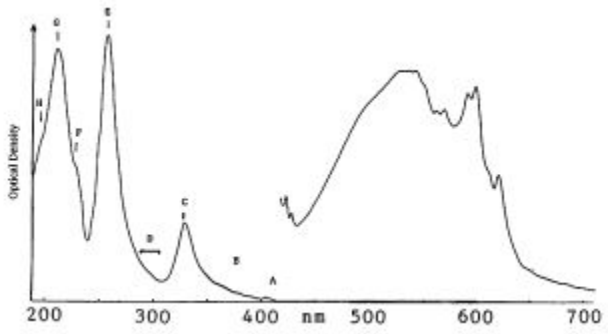

Figure 3.9: A small section of the C_{60} absorption spectrum. The relevant peak at 265 nm can be seen at the peak labeled C. The section of the spectrum on the right has been scaled up to be visible on the same axes, but is actually continuous with the section labeled A. Image credit: [13].

Although there is a strong absorption peak at 265 nm, no response was seen from the spectroscopy setup. This result coupled with the results from the QCM suggest that there is very little C_{60} produced by the back desorption method. More in-depth tests could be performed with both the QCM and spectroscopy setup in order to further verify these results. An optical enhancement cavity could be constructed in order to increase the sensitivity of the spectroscopy measurements, and the QCM could be tested further as discussed previously.

3.2 Front Desorption

The difficulties in developing a back desorption target motivated us to look into front desorption. Laser power is more readily deposited into the analyte which should provide more efficient thermal excitation and subsequent desorption. The disadvantage is a greater possibility of inducing chemical change due to the direct exposure of the analyte to high

optical fluence. We decided to pursue this route nevertheless, since we will eventually do quantum state-resolved spectroscopy of C_{60}, which should be precise enough to filter out other species spectroscopically. In contrast to back desorption, front desorption is a well documented method of producing hydrocarbons for studies in organic and bio chemistry [1]. These methods have been adapted to design the methods presented here to develop a front desorption source of C_{60}.

3.2.1 Target Preparation

Based on the methods reviewed by Rijs et. al, several different methods of producing targets were tested. The first method attempted was a pellet of pure C_{60} made using a hydraulic press. Next, since we are no longer depositing heat through the back of the substrate, a thicker metal backing plate was used instead of metal foils as a substrate for the C60 target. Finally, several different binding agents mixed in with C_{60} were tested as well with varying results.

The targets for front desorption were judged using the same qualitative conditions as the back desorption targets. In addition to these conditions it was also important to ensure that any binding agent or substrate added would not react with the C_{60} and interfere with the yield.

The first targets produced, as mentioned above, were pure C_{60} pellets. These were made using 101,000 - 153,000 psi from a hydraulic press to compress C_{60} powder into a solid pellet. The solid pellets are 12.7 mm in diameter. They are hard and do not break easily, although they will shatter if handled roughly. The C_{60} powder is initially a dusty black color

but forms a shiny surface once compressed. A solid C_{60} pellet can be seen in figure 3.10 (a).

(a) (b)

Figure 3.10: (a) A pellet of pure C_{60} created using a hydraulic press with 127,000 psi. (b) A pellet of reused C_{60} from previous front desorption tests on a copper backing plate, made using a hydraulic press with 10,000 psi

Although they meet all the necessary criteria, the pure C_{60} pellets are relatively expensive to produce and contain an unnecessary amount of C_{60}. In theory all the C_{60} could be desorbed and these targets would have the maximum yield. But, in practice the yield from multiple laser pulses hitting the same spot decreases rapidly with subsequent laser pulses, before the target has been punched through. So, the yield will also decrease as the target is used. Thus, much of the C_{60} in the target will be excess that can't be desorbed.

As mentioned previously, a backing plate was added to press the C_{60} into. The backing plates provide increased mechanical stability. The backing plates used are copper disks 25.4 mm in diameter and 0.635 mm thick. The C_{60} is pressed into the center of the disk using a hydraulic press and a specially made die that holds the copper and C_{60} in place. The die has movable pin to compress the C_{60} into the center of the copper backing plate. Using 10,000 -

25,000 psi from the hydraulic press, the C_{60} forms a very similar disk to the pure pellets in the center of the copper. In order to form a full uniform layer of C_{60} 0.1 $\pm$ 0.01g of C_{60} is required. The entire copper-C_{60} target is put into the desorption setup. A target made this way can be seen in figure 3.10 (b).

When using pure C_{60}, the disk of analyte easily pops out of the copper when handling the target. To mitigate this, different variations of binding agents and C_{60} treatments were tested to find what would adhere the best to the copper backing plates. The binding agents tested were graphite, bismuth, and previously desorbed C_{60}. Both pure C_{60} and previously desorbed C_{60} were used as well. It was found that out of these options the reused C_{60} from previous tests adhered to the copper the most reliably. Pure C_{60} and C_{60} with bismuth powder in a 3:7 (C_{60} : bismuth) ratio by volume were not able to stick to the copper targets at all. Pure C_{60} with graphite in a 3:7 ratio by mass (0.1g total mass) stuck to the copper, but required much higher pressures than the reused C_{60}. The C_{60}-graphite mixture required pressures on the order of 50,000 psi, in contrast to the reused C_{60} which required pressures around 10,000 - 25,000 psi. Additionally, the C_{60}-graphite targets were inconsistent in adhering to the copper. The mechanism causing the reused C_{60} to adhere to the copper so consistently and with such low pressures is unknown and is not within the scope of this paper. Because of the ease of production and availability of material, targets made from reused C_{60} were used for all the data in the following section unless otherwise noted.

3.2.2 Desorption Tests and Yield Characterization

Tests to desorb C_{60} from the targets were conducted using a 532 nm frequency doubled Nd:YAG CW laser. A diagram of the experimental setup can be seen in figure 3.11. An acousto-optical modulator (AOM) was used to pulse the laser. The first AOM diffraction order is focused onto the C_{60} target held inside the vacuum chamber. The desorption laser is swept laterally across the target by using a piezo controlled mirror (M4 in figure 3.11). This allows for continuous scanning of the laser beam across the target. The vacuum chamber is flooded with 6 Torr room temperature Ar gas in order to purge the chamber, preventing combustion and other reactions with air as well as providing collisional quenching of the produced gas. A 265 nm diode laser is passed in front of the target, perpendicular to the YAG laser, as shown in figure 3.11. This is focused onto a photodetector in order to conduct absorption spectroscopy to monitor the output from desorption.

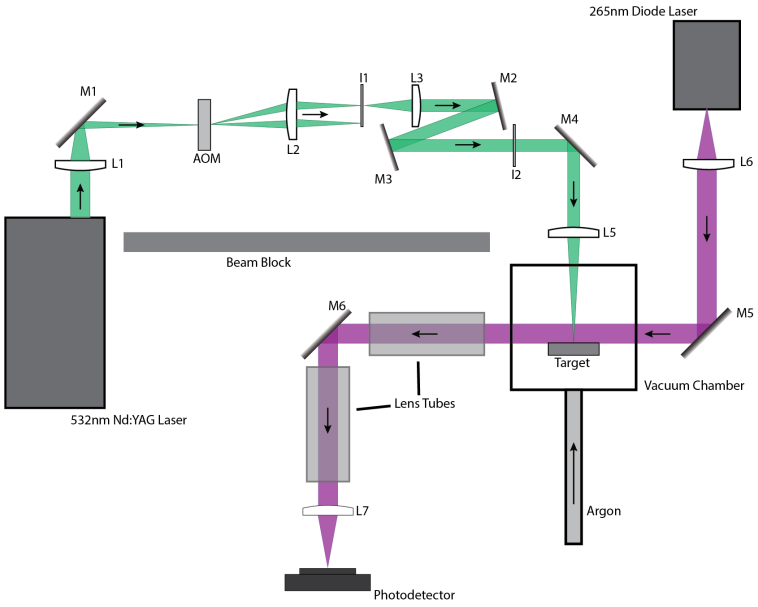

Figure 3.11: The optical setup used to conduct tests on front desorption.

For desorption, a laser fluence of 15.76 mJ/cm^2 from the YAG laser is used. The laser fluence is calculated with the following equation:

$$fluence = \frac{\text{CW Laser power [W]} \times \text{Pulse length [s]}}{\pi(\text{Beam waist [cm]})^2} \tag{3.4}$$

For the desorption tests we utilized 330 mW CW of laser power with a 150 ms pulse duration and estimated a beam waist of 100 μm. Hitting the target with the laser causes the C_{60} to glow an orange color, and when the AOM is pulsed a visible plume of gas comes off the target. This plume suggests there may be a large amount of material coming off the target. To help identify the desorbed material, direct absorption spectroscopy was used. Results from 265 nm spectroscopy can be seen in figure 3.12(a) and from 445 nm in figure 3.12(b). The horizontal axis shows the time in seconds taken to scan across the target using the piezo controlled mirror, the vertical axis shows fractional change from the mean in the photodetector output but is arbitrary for the pulses. The pulses are shown simply to correlate the absorption measurement with the laser pulse.

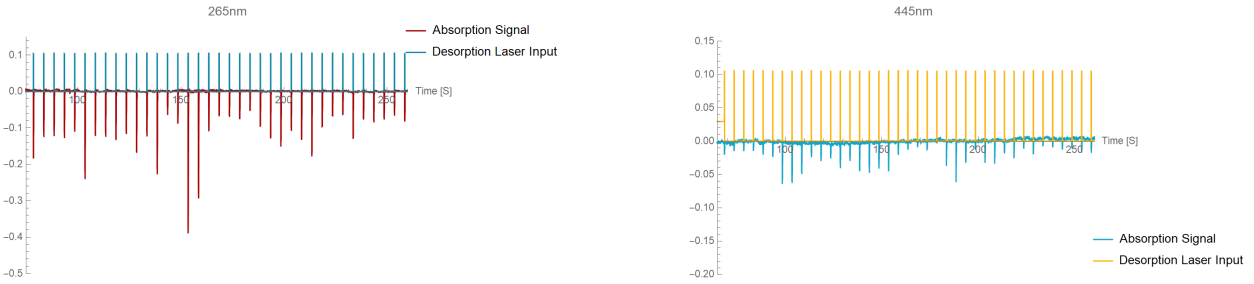

(a) (b)

Figure 3.12: Spectroscopic response and pulse time for 265 nm (a) and 445 nm (b) spectroscopy and pulses from an AOM. The vertical axis shows the fractional change from the mean in the photodetector and is arbitrary for the desorption laser input.

The large absorption response in figure 3.12(a) is consistent with the observations of a

visible gas plume coming off the desorption targets. In order to verify whether the gas being output from the target contained C_{60}, spectroscopy was also done using the same setup at 445 nm, shown in figure 3.12(b).

Based on the absorption spectrum shown in figure 3.9, a much smaller response is expected at 445 nm. The results shown are consistent with this prediction and suggest the presence of molecular C_{60}. Although promising, this is not entirely conclusive. The presence of C_{60} clusters or fragmented molecules with similar absorption lines could give a false positive. In order to verify the presence of molecular C_{60} at least one more wavelength should be tested, or other methods like mass spectrometry could be be preformed. The addition of data from another wavelength would help verify that the absorption response does in fact follow the predicted response for C_{60}. Ideally, a complete spectrum could be done in order to have absolutely conclusive results. Mass spectrometry could be performed on the output and would be able to show the presence of C_{60} based on mass to charge ratios. This would also allow for other compounds in the output to be identified.

Chapter 4

Results and Conclusions

In this thesis, I have presented various methods of gaseous C_{60} production utilizing laser desorption. The goal of these investigations is to minimize or eliminate the limitations on ongoing investigations into the many-body physics of C_{60}. These limitations mainly arise from the method of C_{60} gas production currently in use. The current methods of C_{60} gas production take up to an hour to start producing gas and introduce a large heat load into the system, limiting the maximum time the experiment can be run continuously. Laser desorption presents a promising option as a source of gaseous C_{60} with a very small heat load.

Common methods of laser desorption used in biochemical research have been adapted to suit this purpose, and both front desorption and back desorption sources have been tested. The benefit of a back desorption source is the very low risk of chemical changes and reactions within the C_{60}. On the other hand, front desorption is a well documented method of gas production that provides a solution with simple setup and target production.

The back desorption source did not provide many promising results. Despite qualitative confirmations of desorption, quantitative methods of verifying observations did not indicate any appreciable results. In contrast, front desorption proved to be a suitable method of gas

production that yielded promising preliminary results. Spectroscopic data taken from the gas produced by front desorption have a strong correlation to known absorption spectra of C_{60}, implying there may be a meaningful amount of C_{60} in the output. These results are still preliminary, and more data is needed to confirm that there is a significant amount of molecular C_{60} within the gas produced by front desorption.

Chapter 5

Suggestions for Further Study

In light of the results presented here, several avenues of further study remain open with respect to the validity of laser desorption as a method gaseous C_{60} production. These include further study of the products from both front and back desorption as well as obtaining measurements of the temperature of the gas produced by laser desorption.

Verifying the presence of C_{60} in the products of front and back desorption is necessary to confirm the usefulness of laser desorption as a method of gaseous C_{60} production. The most promising method to verify this is to expand upon the spectroscopic studies presented here. With data from more wavelengths the known spectrum of C_{60} could hopefully be reproduced, creating more confidence in the presence of C_{60}. Alternatively, the resultant gas from desorption could be condensed and, utilizing a C_{60} specific solvent, any molecular C_{60} present could be isolated. The dissolved C_{60} could then be precipitated out of solution, and the amount of C_{60} present could be quantitatively verified from the deposited mass. More in depth spectroscopic studies would be able to isolate the presence of molecular C_{60} in the output gas, in contrast to C_{60} clusters. But, determining the exact amount of C_{60} in the yield would be difficult through this method. In contrast, chemically isolating C_{60} from the condensed gas would allow for quantitative analysis of the amount of C_{60} present. But, this

method may not be able to distinguish molecular C_{60} from C_{60} clusters present in the gas phase.

Because the end goal of laser desorption of C_{60} is a gaseous source of C_{60} for spectroscopic studies, it is important to know the temperature of the resultant gas. If the C_{60} molecules produced by laser desorption are actually much hotter than those produced by the oven, the methods used currently to cool C_{60} into a rovibrational ground state may be insufficient. Although, the low heat load intrinsic to the desorption source means that the gas used to cool the C_{60} within the chamber will stay cooler. This will potentially make it able to cool the hotter C_{60} enough to reach the necessary temperatures for a thermal ground state. So, measuring the temperature of the resultant gas from the desorption source is necessary to determine whether laser desorption will serve as an improvement upon current methods of gas production for C_{60} experiments and whether improvements on the cooling system must be made to integrate it into current experiments.

Bibliography

[1] Sjors Bakels, Marie-Pierre Gaigeot, and Anouk M. Rijs. Gas-phase infrared spectroscopy of neutral peptides: Insights from the far-ir and thz domain. Chemical Reviews, 120:3233–3260, 2020.

[2] P. Bryan Changala. Rovibrational quantum state resolution of the C_{60} fullerene. Science, 363:49–54, 2019.

[3] Yanjun Fang. The functions of fullerenes in hybrid perovskite solar cells. ACS Energy Letters, 2:782 – 794, 2017.

[4] Ol'ga A. Kraevaya. Diversion of the arbuzov reaction: alkylation of $C-Cl$ instead of phosphonic ester formation on the fullerene cage. Organic and Biomolecular Chemistry, 17:7155–7160, 2019.

[5] W. krätschmer. The infrared and ultraviolet absorption spectra of laboratory-produced carbon dust: evidence for the presence of the C_{60} molecule. Chemical Physics Letters, 170:167–170, 1990.

[6] A. Leger. Remarkable candidates for the carrier of the diffuse interstellar bands: C_{60}^{+} and other polyhedral carbon ions. Astronomy and Astrophysics, 203:145–148, 1988.

[7] Lee R. Liu. Collision-induced C_{60} rovibrational relaxation probed by state-resolved nonlinear spectroscopy. PRX Quantum, 3:1–16, 2022.

[8] K. Matsumoto, E. Schönherr, and E. Wojnowski. Growth of C_{60} crystals by the pizzarello method. Journal of Crystal Growth, 135:154–156, 1994.

[9] José Menéndez and John B. Page. Vibrational spectroscopy of C_{60}. `https://www.public.asu.edu/~cosmen/C60_vibrations/newc60revcorr.pdf`.

[10] Ryuichi Mitsumoto. Electronic structures and chemical bonding of fluorinated fullerenes studied by nexafs, ups, and vacuum-uv absorption spectroscopies. J. Chem. Phys. A, 102:552 – 560, 1998.

[11] M. Moalem. Sublimation of higher fullerenes and their interaction with silicon (100) surface. Journal of Physical Chemistry, 99:16736 – 16741, 1995.

[12] David J. Nesbitt and Robert W. Field. Vibrational energy flow in highly excited molecules: role of intramolecular vibrational redistribution. The Journal of Physical Chemistry, 100:12735–12756, 1996.

[13] Giorgio Orlandi and Fabrizia Negri. Electronic states and transitions in C_{60} and C_{70} fullerenes. Photochemical and Photobiological Sciences, 1:289– 308, 2002.

[14] Arthur P. Ramirez. Superconductivity in alkali-doped C_{60}. Physica C: Superconductivity and its Applications, 514:166–172, 2015.

[15] Rodney S. Ruoff, Doris S. Tse, Ripudaman Malhotra, and Donald C. Lorents. Solubility of fullerene (C_{60}) in a variety of solvents. The Journal of Physical Chemistry, 97:3379–3383, 1993.

[16] R. E. Smalley and H. W. Kroto. C_{60}: Buckminsterfullerene. Nature, 318:162–163, 1985.

[17] J. Toscano. private communication, January 2022.